Int. J. Heat Mass Transfer. Vol. 20, pp. 1145–1154. Pergamon Press 1977. Printed in Great Britain

TURBULENCE MEASUREMENTS IN AN AXISYMMETRIC BUOYANT PLUME

WILLIAM K. GEORGE, JR.
State University of New York at Buffalo, N.Y. 14214, U.S.A.

and

RONALD L. ALPERT and FRANCESCO TAMANINI
Factory Mutual Research Corporation Norwood, MA, U.S.A.

(*Received* 7 *May* 1976 *and in revised form* 6 *January* 1977)

Abstract—An experimental investigation of the velocity and temperature fields in an axisymmetric turbulent buoyant plume is described. The plume source was a heated air jet with an exit densimetric Froude number of 1.4. Measurements were carried out with two-wire probes. One wire was maintained at a constant temperature and the other wire was operated as a resistance thermometer. The outputs from both wires were sampled digitally by an *A/D* converter and the temperature and velocity were computed from the experimentally determined calibration curves.

The mean temperature and velocity profiles are presented and compared with previous results obtained by Yih [17]. The profiles of the RMS fluctuating velocity and temperature are also presented along with the velocity–temperature correlations and joint probability distributions. All data show satisfactory agreement with the expected similarity scaling, although there is some evidence in the data for the fluctuating quantities that the plume had not reached a fully developed state.

NOMENCLATURE

a_g, acceleration of gravity;
b, effective plume half width;
d, wire diameter;
E, entrainment rate, $=2\alpha bW$;
F_0, source buoyancy parameter;
g, buoyancy, $=-a_g\Delta\rho/\rho_\infty$;
k, thermal conductivity of fluid;
Nu, Nusselt number [see equation (19)];
q, rate of heat input to constant temperature wire;
R, Reynolds number of flow, $=wd/\nu_f$;
r, radial distance from plume axis;
T, local plume temperature;
ΔT, excess plume temperature, $=T-T_\infty$;
v, local radial plume velocity component;
W, characteristic plume velocity;
w, local vertical plume velocity component;
z, vertical height above source.

Greek symbols

α, entrainment constant;
β, proportionality constant, $=b/z$;
$\Delta\rho$, $\rho-\rho_\infty$;
ρ, local plume density;
η, r/z;
l, wire length;
ν, kinematic viscosity of fluid.

Subscripts

f, film condition evaluated at $(T_w+T_\infty)/2$;
G, gaussian profiles;
GT, gaussian temperature profile;
GW, gaussian velocity profile;
0, source condition;
w, probe-wire condition;
∞, ambient condition of plume environment.

Superscripts

$\bar{}$, time mean;
$\tilde{}$, instantaneous value;
$'$, fluctuating component.

INTRODUCTION

THE TURBULENT buoyant plume has been a subject of investigation for almost forty years (c.f. Zel'dovich [1], Schmidt [2], Taylor [3], Rouse, Yih and Humphreys [4]). While Zel'dovich and Rouse *et al.* proceeded from a similarity hypothesis, Schmidt and Taylor made assumptions about the basic turbulent flow processes. Batchelor [5] independently proposed similarity solutions for turbulent buoyant plumes in both uniform and stratified environments. The similarity solutions are*

$$\bar{w} = F_0^{1/3} z^{-1/3} f_1(r/z) \quad (1)$$

$$\bar{g} = F_0^{2/3} z^{-5/3} f_2(r/z) \quad (2)$$

$$b = \beta z \quad (3)$$

* Following the usual convection, overbars indicate time averages and primes indicate fluctuating components.

where F_0 is the buoyancy produced per unit time at the source and is defined by

$$F_0 = 2\pi \int_0^\infty \overline{wg}\, r\, dr, \tag{4}$$

b is the effective plume width, and g is buoyancy defined by

$$g = -a_g \frac{\Delta\rho}{\rho_\infty} \tag{5}$$

where $\Delta\rho$ is the difference between the local density and that of the ambient fluid.

Morton, Taylor and Turner [6] were able to analyze non-similar flows by invoking a hypothesis which related entrainment rate to local mean velocity. By using the entrainment hypothesis, Morton [7] extended the analysis to plumes arising from sources of buoyancy, mass and momentum and showed that these can be related to equivalent point sources of buoyancy only.

There have been a number of qualitative experiments performed which served to confirm theoretical predictions of maximum height and plume growth rates [9]. The most cited quantitative experiment was by Rouse *et al.* [4] who used vane anemometers and thermocouples to measure mean velocity and temperature profiles in both axisymmetric and two-dimensional plumes in air. The profiles of velocity and buoyancy for the axisymmetric case were given as

$$\bar{w} = 4.7\, F_0^{1/3} z^{-1/3} \exp(-96 r^2/z^2) \tag{6}$$

$$\bar{g} = 11\, F_0^{2/3} z^{-5/3} \exp(-71 r^2/z^2). \tag{7}$$

The width of the temperature profile was observed to be greater than the velocity profile; for the two-dimensional plume, the opposite dependence was found.

Rao and Brzustowski [8] attempted to use a hot wire anemometer to measure turbulence quantities in the plume above a burning wick heat source. The averaged heat-transfer equation for the wire was used with an independent measurement of the mean temperature to calculate both mean and fluctuating velocities. Since the technique discriminates against the hottest and coldest parts of the flow, which correspond to the largest fluctuations in velocity, the measurements are of questionable validity.

In spite of the advances of the past 29 years in flow measurement techniques, the data of Rouse *et al.* remain the basis for theoretical evaluation (c.f. Turner [9], Tennekes and Lumley [10]). The work reported here is a first attempt to use hot wire anemometry in conjunction with digital recording techniques to measure both mean and fluctuating quantities in buoyant plumes.

REVIEW OF BASIC EQUATIONS

It will be instructive to look at the integrated equations of motion for an axisymmetric buoyant plume. We can write (c.f. Turner [9] for a complete discussion) for mass, momentum and buoyancy conservation to within the Boussinesq approximation and for uniform environment

$$\frac{d}{dz} 2\int_0^\infty \bar{w} r\, dr = E \tag{8}$$

$$\frac{d}{dz}\int_0^\infty \overline{w^2} r\, dr = \int_0^\infty \bar{g} r\, dr \tag{9}$$

$$\frac{d}{dz}\int_0^\infty \overline{wg}\, r\, dr = 0 \tag{10}$$

where E is the entrainment rate and will be considered later.

It is commonly assumed that profiles of $\bar{w}$ and $\bar{g}$ are Gaussian. That is

$$f_1 = A \exp[-B\eta^2] \tag{11}$$

$$f_2 = C \exp[-D\eta^2] \tag{12}$$

where $\eta = r/z$ and A, B, C, D are constants. If we ignore the contributions of the fluctuating w velocity to the momentum flux (as is the usual custom) and substitute the assumed Gaussian similarity solution into the momentum equation (equation 9) we obtain

$$\frac{A^2}{B} = \frac{3}{2}\frac{C}{D}. \tag{13}$$

This will be used later in fitting a Gaussian curve to the experimental velocity profile.

The equation for buoyancy conservation tells us that the buoyancy is independent of z; therefore from the definition of equation (10) it follows that buoyancy is given by F_0 at all positions in the plume.

The entrainment rate E is commonly assumed to be proportional to the local velocity scale of the plume. A convenient local velocity scale W and plume width b can be defined from the integrated mass and momentum fluxes as

$$b^2 W = 2\int_0^\infty \bar{w}(r) r\, dr \tag{14}$$

and

$$b^2 W^2 = 2\int_0^\infty \bar{w}^2(r) r\, dr. \tag{15}$$

The entrainment rate E is then defined as

$$E = 2\alpha b W. \tag{16}$$

Substitution of the similarity solution for W into equation (8) immediately yields

$$b = \beta z = \tfrac{6}{5}\alpha z. \tag{17}$$

The parameters b, β and α are unambiguously defined by the equations above. It is common, however, to define the plume half-width in terms of the $1/e$ points of the best Gaussian curve. The relations between these definitions and those above are

$$b_G = b/\sqrt{2}, \quad \beta_G = \beta/\sqrt{2}, \quad \alpha_G = \alpha/\sqrt{2}. \tag{18}$$

EXPERIMENTAL TECHNIQUE

A two-wire probe (DISA P76) was used to obtain "velocity-like" and temperature signals at neighboring locations in the flow (wire spacing $\sim$5 mm). The

temperature signal was obtained by a constant current anemometer (DISA 55M20) operated as a resistance bridge while the "velocity" signal was obtained by a constant temperature anemometer (DISA 55M10). The hot probe was operated at a temperature of 284°C which corresponds to a minimum overheat of 0.5 for the data of this experiment.

The outputs from both anemometers were sampled sequentially with a Hewlett–Packard 2114 computer at a rate of 700 readings per second, converted to digital signals and stored on magnetic tape. Since the sampling rate was approximately an order of magnitude greater than the frequencies corresponding to most of the turbulent energy, the readings were virtually simultaneous. The velocity-temperature calibration curve was then used to calculate the actual velocity signal from the "instantaneous" constant temperature anemometer output. A block diagram of the procedure is shown in Fig. 1.

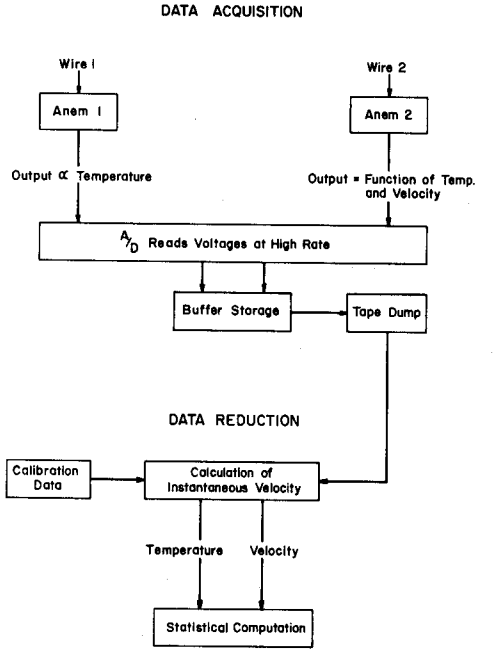

FIG. 1. Block diagram of data acquisition system and data reduction procedure.

CALIBRATION

The temperature–velocity calibration of the probe was obtained using the device shown in Fig. 2. Air is forced through 5 cm of sintered bronze which contains resistive heating elements. The air then passes through two screens (mesh = 0.85 mm, dia = 0.3 mm) and a 15 : 1 contraction. The entire device was sealed in an insulated can to minimize temperature gradients due to heat loss through the walls. The mean temperature variation across the exit was less than 1°C and the velocity and temperature fluctuation levels were less than 0.1%. Mean velocities were obtained by using a total head tube at the exit and by monitoring the bulk flow rate into the settling chamber. Total head tube

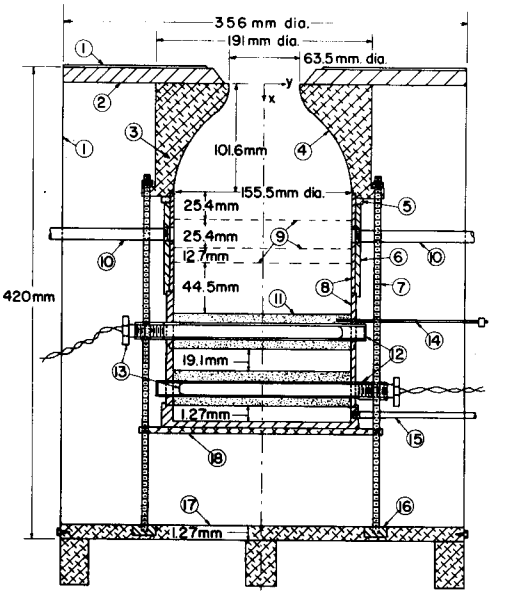

FIG. 2. Schematic of thermal plume generator. (1) Container for silica aerogel insulation, sheet steel. (2) Cerafelt insulation; 1.27 mm thick. (3) Aluminum exit nozzle. (4) Inner aluminum surface machined approximately to:

$$y = 31.75 + 2.42 \times 10^{-8} X^5 - 6.1 \times 10^{-6} X^4 + 4.36 \times 10^{-4} X^3 \text{ (mm)}.$$

(5) Gasket; RTV-106 (General Electric). (6) Bearing bronze sleeve; approximately 0.6 mm wall thickness; sealed to part No. 8 with RTV-106. (7) Three threaded rods spaced 120° apart, 0.8 mm dia, for sealing exit nozzle and supporting entire system in aerogel insulation. (8) Copper pipe. (9) Copper screens, sealed to segments of part No. 8 with RTV-106; 1.18 wires/mm; wire dia 0.305 mm. (10) Two entry pipes threaded into part No. 6 to allow for insertion of probes or for pressure measurement. (11) Two sintered bronze castings; 31.8 mm thick, density 4.5–5 g/cm^3; will allow passage of particles smaller than 150 μ dia; thermet grade 12 HP. (12) Eight copper pipes cast into sintered bronze, sealed with RTV-106 to outer surface of part No. 8; 9.55 mm ID; In upper part No. 11, pipes are evenly spaced across sintered bronze and aligned paralell to air inlet pipe, No. 15; In lower part, No. 11, 4 pipes are evenly spaced across sintered bronze and aligned perpendicular to air inlet pipe, No. 15. (13) Eight electric heaters, one each copper pipe No. 12, adjacent heaters facing opposite directions; Watlow Firerod C6A81, 110 V, 400 W each; 9.55 mm dia, 153 mm long; brass pipe-thread fitting with ceramic bead insulation on lead wires; high temperature copper–graphite–lead compound (Kopr-Kote by Jet-Lube) fills any space between heater and wall of copper pipe No. 12. (14) Two thermocouple probles, one each part No. 11, sealed with RTV-106 to outer surface of part No. 8; Omega CAIN-116U-12. (15) Air inlet pipe. (16) Phenolic plugs. (17) Aluminum base plate on three aluminum feet.

measurements were corrected for buoyancy effects on the tube. Flow velocities could be varied from 10 cm/s to 10 m/s and exit temperatures in excess of 300°C were obtainable.

Over the range of velocities of this experiment, a logarithmic calibration was found to provide the best fit to the experimental data. This is consistent with those of Collis and Williams [11], who showed that a logarithmic relation is superior for probe Reynolds numbers below 0.5.

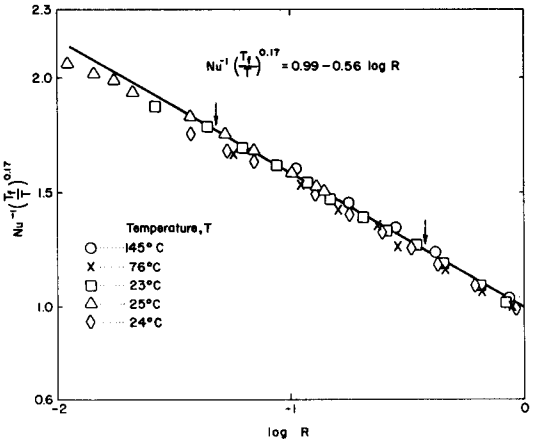

FIG. 3. Velocity probe calibration curve.

The calibration curve for the probe used in the measurements is shown in Fig. 3. The Nusselt number is defined as

$$Nu = \frac{q}{\pi k_f l (T_w - T)} \tag{19}$$

where q is the resistive heating and k_f is the thermal conductivity of the fluid at the film temperature. The temperature loading factor of Collis and Williams [11] was used in the data shown. A least square fit to the data yielded

$$Nu^{-1}\left(\frac{T_f}{T}\right)^{0.17} = A_1 - B_1 \log R \tag{20}$$

where $A_1 = 0.99$ and $B_1 = 0.56$. (Note that these are different from the values obtained by Collis and Williams because of the shorter length to diameter ratio of the wires $l/d \sim 200$.) The scatter in the calibration is believed to be primarily due to thermal effects on the total head tube; the slight roll off at lowest velocities could be due to either viscous effects on the total head tube or the onset of free convection on the wire (c.f. Hollasch and Gebhart [12], Warpinski *et al.* [13]). In either case, it is below the range of velocities encountered in this experiment.

EXPERIMENTAL ERRORS

Measurement errors stemmed from two basic causes: first, the thermal inertia of the temperature wire, and second, the directional ambiguity of the hot wire. Statistical error was less than 3% in the velocity and even lower for the mean and rms quantities. The resolution limitation imposed by the wire separation corresponded to a length about twice the Kolmogorov microscale and was minimal compared to the cutoff due to thermal inertia.

The frequency response of the temperature wire was estimated to be about 300 Hz (from Hinze [14]). For comparison, the estimated frequency of the energy containing eddies was less than 50 Hz and that of the Kolmogorov microscale was about 1 kHz. Since the velocity wire was operated at constant temperature, its frequency response was orders of magnitude better than the cold wire. In order to avoid the possibility of measuring rapid velocity changes induced by rapid thermal fluctuations which the temperature probe could not follow, the velocity signal was low-passed electronically at 350 Hz. This was not felt to significantly affect the statistics reported.

The directional ambiguity of the hot wire presents a more serious problem. The wire responds equally to both components of velocity perpendicular to it; therefore, the effective cooling velocity is

$$\tilde{q}^2 = \tilde{w}^2 + \tilde{v}^2 \tag{21}$$

where $\tilde{}$ denotes the instantaneous value. It is straightforward to show via a binomial expansion that the mean cooling velocity is given by

$$\bar{q} = \overline{[(\bar{w}+w')^2 + (\bar{v}+v')^2]^{1/2}} \simeq \bar{w}\left\{1 + \frac{1}{2}\frac{\bar{v}^2 + \overline{v'^2}}{\bar{w}^2}\right\} \tag{22}$$

where third order terms have been neglected. The mean square fluctuating velocity, similarly, can be calculated as

$$\overline{q'^2} = \overline{\tilde{q}^2} - \bar{q}^2 \simeq \overline{w'^2}\left\{1 + \frac{\overline{w'^3}}{\bar{w}\overline{w'^2}} + 2\frac{\overline{w'v'}\bar{v}}{\overline{w'^2}\bar{w}} + \frac{\overline{w'v'^2}}{\bar{w}\overline{w'^2}}\right\}. \tag{23}$$

Clearly, these inaccuracies will dominate at the outer edge of the plume where the relative velocity fluctuations are high.

It should be noted that because of the data conversion techniques used, the velocity computed is the actual velocity the probe sees and is not subject to the usual non-linearities associated with hot wires (c.f. Hinze [14]).

THE EXPERIMENTS

The calibrator described earlier was used as a heat source for the axisymmetric plume experiment. The source temperature was 300°C and the exit velocity was 67 cm/s (calculated from measured heat flux). The entire apparatus was placed in a square shelter 2.44 $\times$ 2.44 $\times$ 2.44 mm. Air was allowed to enter along a 5 cm baffled gap along the floor and the plume exited through a 46 cm dia hole in the roof. The laboratory was air conditioned and specially designed to eliminate cross drafts in the room. The ambient air temperature remained at 29 ± 1°C.

Flow visualization was achieved by injecting smoke into the plenum chamber of the calibrator. There was no evidence of plume wandering, either visually or in the data reported below.

The source exit conditions correspond to a Reynolds number of 870 and a densimetric Froude number of 1.4. There was no evidence of laminar behavior above a distance of 2 exit diameters.

EXPERIMENTAL RESULTS

Measurements of mean and fluctuating quantities were taken at distances of 0.508, 0.762 and 1.016 m above the source. When non-dimensionalized by the

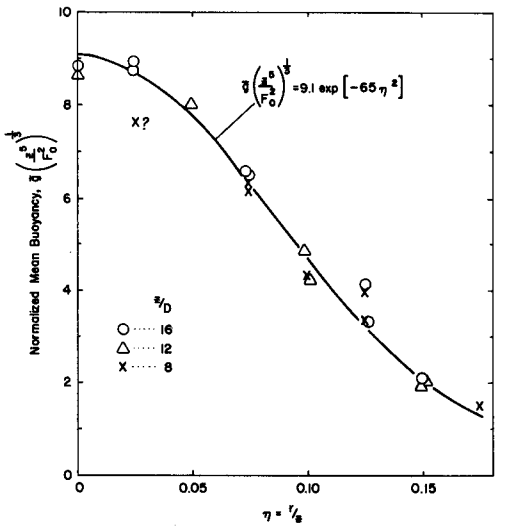

FIG. 4. Mean buoyancy radial profile.

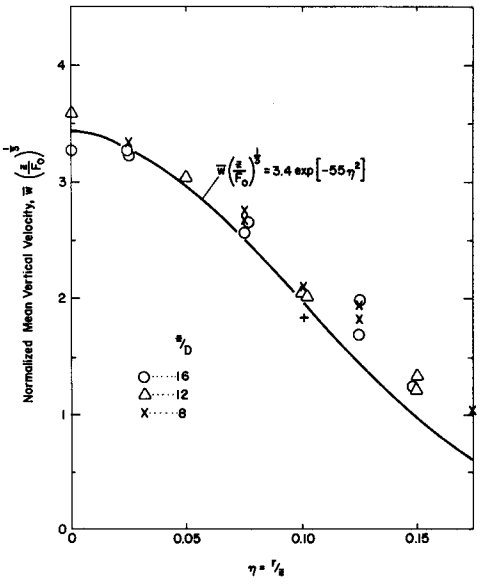

FIG. 5. Mean vertical velocity radial profile.

source diameter, 6.35 cm, these correspond to $z/D = 8$, 12, and 16 respectively. The effective origin of the plume was verified to be in the plane of the exit by several means (see Appendix A).

Mean temperature and velocity profiles are shown in Figs. 4 and 5. The data have been normalized by the buoyancy parameter, F_0, which was found to be 1.0 $\times 10^6$ cm^4/s^3 by integrating the heat flux (including the turbulent contribution!) across the various axial stations. It is clear that both profiles are self-preserving.

A least squares fit to the temperature profile yields

$$\bar{g} = 9.1\, F_0^{2/3} z^{-5/3} \exp[-65 r^2/z^2]. \qquad (24)$$

The exponent is close to that observed by Rouse *et al.* [equation (7)]. The difference in the coefficient is in part due to the fact that in this case account was taken of the near 15% turbulent heat transport.

A plot of the temperature profile on the velocity data reveals that the latter is broader. This is contrary to the findings of Rouse *et al.*, who found the velocity profile to be narrower by 30%. The plus sign at the $1/e$ point in Fig. 5 shows the lowest value that the velocity could have if the correction of equation (22) is applied using the measured value of $\bar{w}'^2$, assuming that $\bar{v}'^2 \leqslant \bar{w}'^2$, and substituting for $\bar{v}$ in equation (22) the similarity form obtained from mass conservation. It is clear that the correction is considerably less than would be necessary to substantiate the earlier results.

The arrows in Fig. 3 denote the velocity range over which the data were taken. Since the only parameters in the calibration are intercept and slope, the lowest values of velocity are subject to proportionally greater error. A conservative estimate of this error based on the variance of the calibration curve is less than 20% at the lowest velocity measurement. Thus, the deviation from Rouse's results cannot be attributed entirely to our calibration error. Near the centerline for which the calibration is optimal and the directional ambiguity low, the estimated error from all sources is less than 5%.

In view of the high confidence level of the centerline velocity data and of the temperature fit [equation (24)], the best estimate of a Gaussian velocity curve is obtained from the constraints imposed by the momentum equation [equation (13)]. Using $C = 9.1$, $D = 65$, and $A = 3.4$ we obtain $B = 55$, and the appropriate Gaussian curve is given by

$$\bar{w} = 3.4\, F_0^{1/3} z^{1/3} \exp[-55 r^2/z^2] \qquad (25)$$

which can be compared with the results of Rouse *et al.* in equation (6). Thus the velocity profile is wider than the temperature profile by about 10%. Because of the dependence of equation (13) on the square of the centerline velocity, the temperature and velocity profiles could be assumed equal to within experimental error. It should be noted that there is no *a priori* reason why the curve should even be Gaussian.

The appropriate similarity forms for the turbulent fluctuations of temperature and vertical velocity are given by

$$(\overline{w'^2})^{1/2} = F_0^{1/3} z^{-1/3} f_3(r/z) \qquad (26)$$

and

$$a_g \frac{(\overline{T'^2})^{1/2}}{\bar{T}} = F_0^{2/3} z^{-5/3} f_4(r/z). \qquad (27)$$

Values of RMS w and T obtained from the dual-wire measurements are shown in Figs. 6 and 7, non-dimensionalized by the centerline values of $\bar{w}$ and $\overline{\Delta T}$, respectively ($\Delta T = T - T_\infty$). Except for slight departures from similarity near the center, the predicted scaling is generally satisfactory. This is particularly gratifying in view of the proximity to the source ($8 < z/D < 16$). Nonetheless, there is clear evidence that the flow is still developing. Noteworthy by its absence is the strong off-axis peak in the profile of the scalar fluctuations usually observed in forced convection jets (c.f. Becker *et al.* [15]).

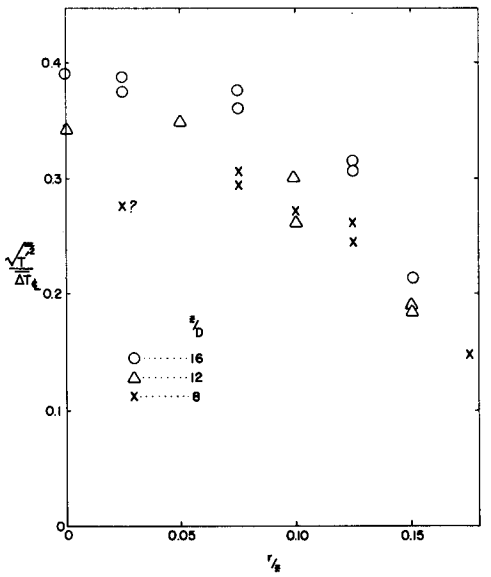

FIG. 6. Radial distribution of intensity of temperature fluctuations.

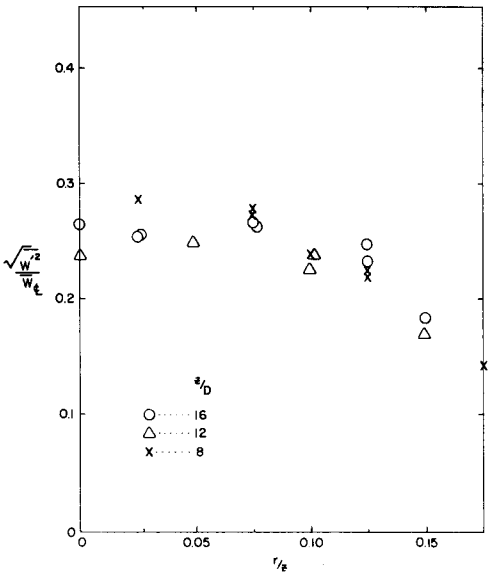

FIG. 7. Radial distribution of intensity of vertical velocity fluctuations.

Application of equation (23) using measured values of skewness and turbulence intensity indicate a centerline overestimate due to directional ambiguity of less than 20%. A similar estimate at $r/z = 0.1$ indicates the measured value of $(\overline{w'^2})^{1/2}$ may be too high by as much as 40%.

It is interesting to note the values of rms temperature and velocity compared to the mean temperature difference (between plume and environment) and mean velocity, respectively. At the centerline

$$\frac{(\overline{T'^2})^{1/2}}{\Delta T} \sim 0.40 \tag{28}$$

and

$$\frac{(\overline{w'^2})^{1/2}}{\bar{w}} \sim 0.28. \tag{29}$$

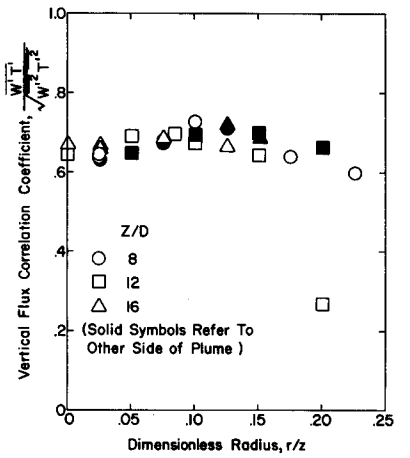

FIG. 8. The velocity–temperature correlation coefficient.

Clearly, the relative fluctuations are in no sense small!

In a plume dominated by buoyancy, one would expect substantial velocity fluctuations to be caused by temperature fluctuations, thus resulting in a high correlation coefficient. Calculations of the correlation coefficient from the data at all measurement locations are summarized in Fig. 8. It is clear that

$$\frac{\overline{w'T'}}{(\overline{w'^2})^{1/2}(\overline{T'^2})^{1/2}} \sim 0.6\text{–}0.7.$$

Within experimental error, the coefficient may be assumed constant at the average value of 0.67. This value is significantly greater than that usually obtained for heated forced jets and is evidence of the important role of buoyancy in the structure of plume turbulence.

Figures 9 and 10 show the probability distributions of temperature and velocity at the highest location at which measurements were made ($z = 1.016$ m). The large intermittency at the outer edge is evident from the highly skewed distributions for $r/z = 0.15$.

Figure 11 shows a contour plot of temperature–velocity joint probability density function on the axis of the plume at $z = 1.016$ m. The strong influence of buoyancy is evident from the diagonal ridge on the map. Also shown is the bivariate normal distribution having a correlation coefficient of 0.67. This appears to adequately model the turbulence to within two standard deviations.

DISCUSSION

Profiles of the mean and RMS fluctuating temperature and axial velocity were measured in a turbulent plume generated by rising hot air. The measured mean temperature profile showed good agreement with Gaussian profiles obtained by Rouse *et al.* [4]. The velocity profile was found to be wider than the temperature profile and the centerline value lower, contrary to the earlier results. The difference could not be attributed to our experimental error.

The data can be used to evaluate the constants in equations (16)–(18). From the Gaussian curve fits we obtain

$$b_{GT} = 0.124\,z, \quad b_{GW} = 0.135\,z. \tag{30}$$

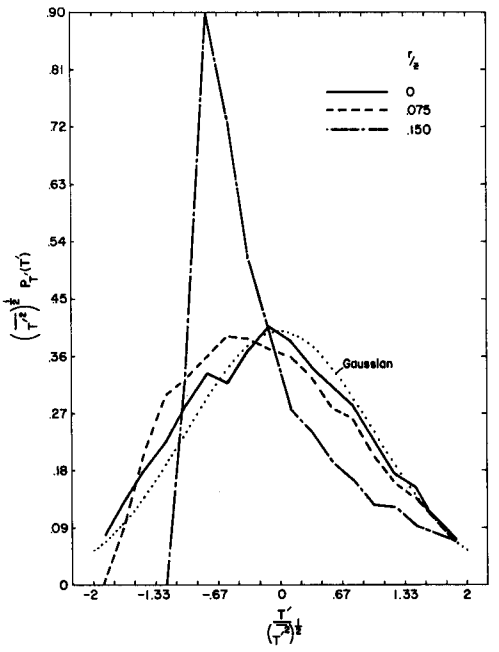

FIG. 9. Normalized probability density distribution of temperature fluctuations at three radial locations for $z = 1.016\,m$.

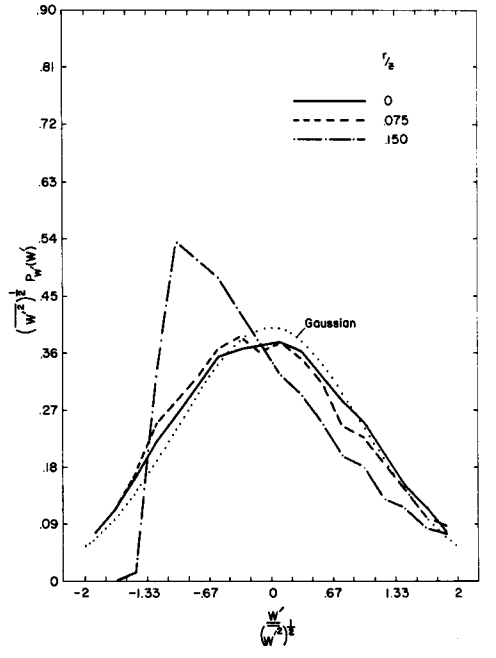

FIG. 10. Normalized probability density distribution of vertical velocity fluctuations at three radial locations for $z = 1.016$ m.

Thus to within experimental error

$$b_G \cong 0.13z, \quad \text{or} \quad b = 0.18z. \tag{31}$$

We can immediately obtain the entrainment constant as

$$\alpha_G = 0.108, \quad \text{or} \quad \alpha = 0.153. \tag{32}$$

The value of $\alpha = 0.15$ obtained here is considerably higher than that used by Morton [7] who adopted a

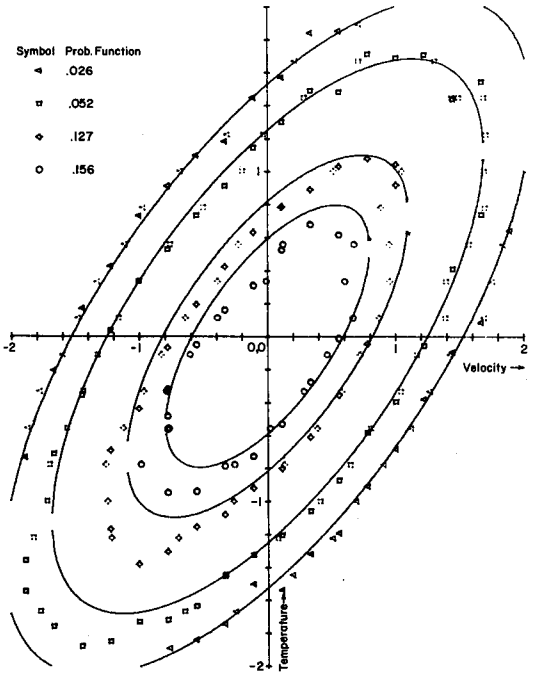

FIG. 11. Temperature–velocity joint probability density function on the axis of the plume at $z = 1.016$ m.

value of 0.116 based on the available literature. Ricou and Spalding [16], used a direct method of measuring entrainment to obtain a value of 0.08 in forced jets. Turner [9] suggests that the entrainment rate in plumes is probably greater than in jets but less than the value of 0.12 previously used. Thus, these measurements are at considerable variance with the previous results.

A careful analysis of the hot wire calibration errors and experimental procedures does not reveal the reasons for these discrepancies. The collapse of the data at large r/z indicates the absence of systematic errors. The large scale meandering of the plume often present in plume experiments was not detectable from smoke injection studies nor was there evidence of plume wandering in the temperature measurements.

The previous measurements reported by Yih [17] and Rouse *et al.* [4], on the other hand, could be in error, both because of the experimental techniques and the manner in which the flow was generated. Temperature difference measurements were made with a thermocouple, normally considered satisfactory for such flows. It is not surprising then that these measurements show the least discrepancy with those reported here. The velocity measurements were made with a vane anemometer (3 cm dia) which had a lower velocity limit of about 6 cm/s. The accuracy of such an instrument in highly turbulent flows is certainly considerably less than those used in the present measurements. A final source of discrepancy could result from the manner in which Yih's flow was generated; namely, a gas burner. Since the burner is primarily a heat source it could require considerable distance to develop the necessary momentum to achieve a fully

developed state. The flow used in this investigation, on the other hand, was generated by forced hot air with source densimetric Froude number near unity. Thus the momentum and heat flux appropriate to a fully developed plume were provided and only a readjustment of the profiles and intensities was necessary to achieve the asymptotic state. These observations on source difference are consistent with the fact that both Yih's centerline temperature and velocity are larger than those reported here, and the velocity profile is considerably narrower.

Townsend [18] argues that the temperature profile should be narrower than the velocity profile since the excess temperature is found only in the turbulent fluid and will therefore behave as the velocity gradient which is wider. Lumley [19] shows that because of a stable temperature gradient at the outer edge of the turbulent plume, the large eddies are compressed vertically and extended laterally. It follows that the mean velocity gradient in the radial direction is reduced, the mean velocity profile is broadened and the flow spreads more rapidly than the non-buoyant jet. Thus Townsend's argument can still be valid; only the conclusion is different.

Measurements have also been reported of the RMS temperature and vertical velocity fluctuations as well as their correlation (Figs. 6 and 7). Both temperature and velocity fluctuations exhibit a reasonably constant value over the center portion of the plume. It is interesting to compare these results with those obtained in isothermal axisymmetric jets by Wygnanski and Fiedler [20] and Becker *et al.* [15].

The radial distribution of the axial component of the turbulence intensity, $(\overline{w'^2})^{1/2}/\bar{w}_c$, measured by Wygnanski and Fiedler is similar to the one shown in Fig. 7, both qualitatively and quantitatively. This result might appear rather surprising. One possible explanation is that in the thermal plume, the additional generation of turbulence due to the action of buoyancy $[a_g(1/T_0)\overline{w'T'}]$ is partially balanced by a smaller (than in the forced jet) contribution from the secondary components of strain $[-\overline{w'^2}(\partial\bar{w}/\partial z)-\overline{v'^2}(\partial\bar{v}/\partial r)]$. Note, that, while $\bar{w}$ decays as z^{-1} in a forced jet, the mean velocity in the plume decays as $z^{-1/3}$.

By assuming that small temperature differences behave in the same way as species concentrations, the data in Fig. 6 can be compared directly with the measurements of the mean and fluctuating concentration of a marker fluid in an axisymmetric isothermal air jet reported by Becker *et al.* [15]. They show that the radial profile of the intensity of the concentration fluctuations has an off-axis maximum (for $\eta \simeq 0.08$) which is about 15% higher than the axis value. Furthermore, the asymptotic value of the fluctuation intensity referred to the local mean concentration was measured by Becker *et al.* to be 0.22 at $\eta = 0$. This is a much lower value than the 0.37–0.38 of Fig. 6.

A tentative explanation of this difference can be given by considering the role of the secondary components of the spacial gradient in the generation of fluctuations. The term representing production of $\overline{T'^2}$ can be written as

$$P_{T'} = -2\overline{w'T'}\frac{\partial \bar{T}}{\partial z} - 2\overline{v'T'}\frac{\partial \bar{T}}{\partial r}. \tag{33}$$

In a forced jet the first term is probably negligible with respect to the second (which has an off-axis maximum). The situation is different in a thermal plume for two reasons. First, the longitudinal heat flux $\overline{w'T'}$ is larger, because of the high correlation of the two variables w' and T' caused by buoyancy. Second, the longitudinal gradient $\partial \bar{T}/\partial z$ becomes important since $\Delta \bar{T}$ decreases as $z^{-5/3}$ instead of the z^{-1} dependence of the forced jet. The lack of an off-axis peak in the data in Fig. 6 is therefore attributed to increased contribution from the first term of equation (33). All these considerations need to be confirmed by additional measurements. A more detailed investigation of the turbulent energy balance is currently being carried out by one of the authors (WKG).

Finally, it is worth noting the effect of the turbulent quantities on the vertical transport of momentum and buoyancy. While less than 8% of the vertical momentum transport is due to the turbulent fluctuations, nearly 15% of the vertical heat transport is due to the turbulent contribution. Clearly, this can hardly be considered negligible.

Acknowledgements—The authors are grateful to Dr. John de Ris of Factory Mutual Research for valuable counsel throughout the investigation, Mr. N. F. Todtenkopf and Ms. Mary Mathews of Factory Mutual who labored many hours preparing programs and editing data and to Ms. Denise Everitt of SUNYAB who assisted with the data analysis and provided many helpful comments. The assistance of Mr. Ron Humphrey and the DISA staff throughout the investigation is also gratefully acknowledged.

The measurements reported here were performed at the Factory Mutual Research Corporation while the first author (WKG) was on a 1974 summer research appointment. Support for WKG during the final stages of this investigation was provided by the New York State Science and Technology Foundation and the SUNY Research Foundation.

REFERENCES

1. Ya. B. Zel'dovich, Limiting laws for turbulent flows in free convection, *Zh. Eksp. Teoret. Fiz.* **7** (12), 1463 (1937).
2. W. Z. Schmidt, Turbulent propagation of a stream of heated air, *Z. Angew. Math. Mech.* **21**, 265–351 (1941).
3. G. I. Taylor, Dynamics of a mass of hot gas rising in air, U.S. Atomic Energy Commission, MDDC, 919, LADC 276 (1945).
4. H. Rouse, C. S. Yih and H. W. Humphreys, Gravitational convection from a boundary source, *Tellus* **4**, 201 (1952).
5. G. K. Batchelor, Heat convection and buoyancy effects in fluids, *Q. Jl. R. Met. Soc.* **80**, 339–358 (1954).
6. B. R. Morton, G. I. Taylor and J. S. Turner, Turbulent gravitational convection from maintained and instantaneous sources, *Proc. R. Soc.* **234A**, 1–23 (1956).
7. B. R. Morton, Forced plumes, *J. Fluid Mech.* **5**, 151–163 (1959).
8. V. K. Rao and T. A. Brzustowski, Preliminary hot-wire measurements in free convection zones over model fires, *Combust. Sci. Technol.* **1**, 171–180 (1969).
9. J. S. Turner, *Buoyancy Effects in Fluids.* Cambridge University Press, Cambridge (1973).
10. H. Tennekes and J. L. Lumley, *A First Course in Turbulence.* MIT Press, Cambridge (1972).

11. D. C. Collis and M. J. Williams, Two dimensional convection from heated wires at low Reynolds numbers, *J. Fluid Mech.* **6**, 357 (1959).
12. K. Hollasch and B. Gebhart, Calibration of constant-temperature hot-wire anemometers at low velocities in water with variable fluid temperature, *J. Heat Transfer* **94** (1), 17–22 (1972).
13. N. R. Warpinski, H. M. Nagib and Z. Lavan, Experimental investigation of recirculating cells in laminar coaxial jets, *AIAA Jl* **10** (9), 1204–1210 (1972).
14. J. Hinze, *Turbulence: An Introduction to Its Mechanism and Theory*. McGraw-Hill, New York (1959).
15. H. A. Becker, H. C. Hottel and G. C. Williams, The nozzle-fluid concentration field of the round, turbulent, free jet, *J. Fluid Mech.* **30**, 285–303 (1967).
16. F. P. Ricou and D. B. Spalding, Measurements of entrainment by axisymmetric jets, *J. Fluid Mech.* **11**, 21–32 (1961).
17. C. S. Yih, Free convection due to boundary sources, *Fluid Models in Geophysics, Proceedings of the First Symposium on the Use of Models in Geophysical Fluid Dynamics, The Johns Hopkins University, Baltimore, Md.*, edited by R. R. Long (1953).
18. A. A. Townsend, *The Structure of Turbulent Shear Flow*. Cambridge University Press, Cambridge (1956).
19. J. L. Lumley, Explanation of thermal plume growth rates, *Physics Fluids* **14**, 2537 (1971).
20. I. Wygnanski and H. Fiedler, Some measurements in the self-preserving jet, *J. Fluid Mech.* **38**, 577–612 (1969).

APPENDIX A

Choice of Origin for Plume Data

The similarity relations for velocity and temperature yield

$$\bar{w} \propto (z-z_0)^{-1/3}$$

and

$$\overline{\Delta T} \propto (z-z_0)^{-5/3}$$

where z_0 is the effective origin and z is measured from the source. It follows that

$$\bar{w}^3 z = K_1 + \bar{w}^3 z_0$$

and

$$\overline{\Delta T}^{3/5} z = K_2 + \overline{\Delta T}^{3/5} z_0$$

where K_1, K_2 are constants. The origin z_0 is thus seen to be the slope of a plot of $\overline{\Delta T}^{3/5} z$ vs $\overline{\Delta T}^{3/5}$ or $\bar{w}^3 z$ vs $\bar{w}^3$. The temperature version should yield more reliable results since measurement errors are reduced by the radical whereas for the velocity they are magnified threefold. A plot of the center line temperature data yielded $z_0 = 0 \pm 5$ cm. Since the nearest axial point was 50 cm, the origin was chosen at the level of the exit plane.

Morton [7] has shown that a forced plume can be treated as a virtual point source of buoyancy located at some distance below the actual source position. Application of equation (11) of Morton [7] to the data at the three axial positions yields a virtual origin position within the limits determined experimentally, thus, providing additional confirmation for the choice.

MESURES DE TURBULENCE DANS UN PANACHE AXISYMETRIQUE

Résumé—On décrit une étude expérimentale des champs de vitesse et de température dans un panache axisymétrique et turbulent. La source est un jet d'air chaud avec un nombre de Froude de 1,4. Les mesures sont effectuées avec des sondes à deux fils. Un fil est maintenu à température constante et l'autre fonctionne en thermomètre à résistance. Les signaux de sortie des fils sont traités digitalement par un convertisseur *A/D* et les températures et les vitesses sont calculées à partir des courbes expérimentales d'étalonnage.

Les profils de température et de vitesse moyennes sont présentés et comparés avec des résultats antérieurs obtenus par Yih [17]. Les profils des moyennes quadratiques des vitesses et des températures sont donnés avec les corrélations et les distributions de probabilité. Tous les résultats donnent un accord satisfaisant avec la représentation en similitude bien que les quantités fluctuantes montrent que le panache n'a pas atteint un état pleinement établi.

TURBULENZMESSUNGEN IN EINER ROTATIONSSYMMETRISCHEN AUFTRIEBSSTRÖMUNG

Zusammenfassung—Es wird die experimentelle Untersuchung des Geschwindigkeits- und Temperaturfeldes in einem turbulenten, rotationssymmetrischen Auftriebsstrahl beschrieben. Als Auftriebsquelle diente ein beheizter Luftstrahl mit einer mit den Dichten gebildeten Austritts–Froude–Zahl von 1,4. Die Messungen wurden mit Doppeldrahtsonden durchgeführt. Ein Draht wurde auf konstanter Temperatur gehalten, der andere diente als Widerstandsthermometer. Die Meßwerte wurden über einen Analog-Digital-Umsetzer digital aufgenommen; Temperatur und Geschwindigkeit wurden aus den experimentell ermittelten Eichkurven berechnet. Die Profile der mittleren Temperaturen und Geschwindigkeiten werden angegeben und mit früheren Ergebnissen von Yih [17] verglichen. Die Profile der mittleren Schwankungsgeschwindigkeiten und -temperaturen werden zusammen mit den Geschwindigkeits-Temperatur-Korrelationen und der Verbund-Wahrscheinlichkeitsdichte ebenfalls angegeben. Alle Werte zeigen befriedigende Übereinstimmung mit der erwarteten Aehnlichkeitsdarstellung, obwohl die Daten für die Schwankungsgrößen andeuten, daß die Auftriebsströmung noch nicht den voll ausgebildeten Zustand erreicht hatte.

ИЗМЕРЕНИЕ ТУРБУЛЕНТНОСТИ В ОСЕСИММЕТРИЧНОЙ СВОБОДНОКОНВЕКТИВНОЙ СТРУЕ

Аннотация — Описывается экспериментальное исследование скоростных и температурных полей в осесимметричной турбулентной свободноконвективной струе. Источником служила струя нагретого воздуха с числом Фруда на выходе, равном 1.4. Измерения проводились с

помощью двухниточных датчиков. Одна из нитей служила датчиком термоанемометра постоянной температуры, а вторая — датчиком термометра сопротивления. Выходные сигналы обоих приборов преобразовывались с помощью аналого-цифрового преобразователя в цифровую, а температура и скорость рассчитывались по калибровочным кривым, построенным на основании экспериментальных данных. Приводятся профили средней температуры и скорости и дается сравнение с результатами, полученными Уайя [17]. Также приведены профили среднеквадратичных значений пульсаций скорости и температуры, а также корреляции скорости и температуры и совместные распределения вероятности. Все данные удовлетворительно согласуются с рассчитываемыми автомодельными характеристиками, хотя некоторые из данных для пульсационных величин свидетельствуют о том, что струя не достигает полностью развитого состояния.